The thermolytic behaviour of hexa-1,5-diene-units incorporated in a stellane and twistbrendane skeleton. A quest for a stepwise Cope rearrangement

Holger Lange, Patrick Loeb, Thilo Herb and Rolf Gleiter *

Organisch-Chemisches Institut der Universität Heidelberg, Im Neuenheimer Feld 270, D-69120 Heidelberg, Germany

The thermolytic behaviour of the tricyclo[3.3.0.0³,⁷]octane (stellane) derivatives 11–13 as well as the tricyclo-[4.3.0.0³,⁸]nonane (twistbrendane) derivatives 14 and 15 have been investigated in d_8-toluene. All five compounds undergo Cope rearrangements to the tricyclic systems 16–20. By means of ^1H NMR spectroscopy the kinetics of these reactions have been studied at different temperatures. The lowest activation energies were encountered for the reactions of 12 and 13 (27.0 and 26.3 kcal mol^{-1}, respectively). Model calculations on the RHF and CASSCF level and beyond (CASPT2N/6-31G*//RHF/6-31G*; CASPT2N/6-31G*//CASSCF/6-31G*) were performed for the rearrangements of 11→16, 13→18, and 27→28. These calculations reveal that the activation energies for the two-step pathway and the concerted pathway are very similar. In the case of 11 and 27 the two step mechanism via a bisallylic diradical intermediate is predicted to be slightly preferred.

The thermal rearrangement of hexa-1,5-diene (1) discovered in 1940 by Cope and Hardy[1] has been the subject of extensive experimental[2] and theoretical[3–5] investigations. For hexa-1,5-diene one can envisage several possibilities: a synchronous one-step mechanism via an aromatic 6π transition state (b) (see Scheme 1); or a cyclohexane-1,4-diyl (c) or two allylic radicals
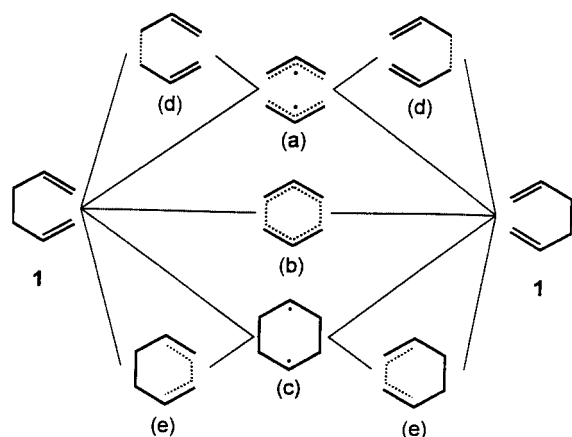

Scheme 1 Possible routes for the Cope rearrangement of hexa-1,5-diene.

(a) as intermediates or transition states. In the case of a step-wise mechanism via a or c the corresponding transition states are d and e, respectively.

The various possibilities listed in Scheme 1 are also met in reality. By using the secondary kinetic isotope effect on phenyl- and cyano-substituted hexa-1,5-dienes, it has been shown that phenyl groups in 2 and 5 positions stabilize the cyclohexane-1,4-diyl structure while cyano groups in the 3 position lower the energy of the bisallylic intermediate.[6,7]

There are also Cope rearrangements which proceed via a biradical intermediate. Extensive studies by Roth et al.[8,9] have demonstrated that the energy of the path via c can be lowered by methylidene- or phenyl-groups. It was shown that the differ-ence in activation enthalpy between a concerted path and a

stepwise path for hepta-1,2,6-triene (2)[8] and octa-1,2,6,7-tetraene (5)[8] is only 2.0 kcal mol^{-1} and 1.5 kcal mol^{-1}, respect-ively (Scheme 2). Trapping experiments on 2 indicate two
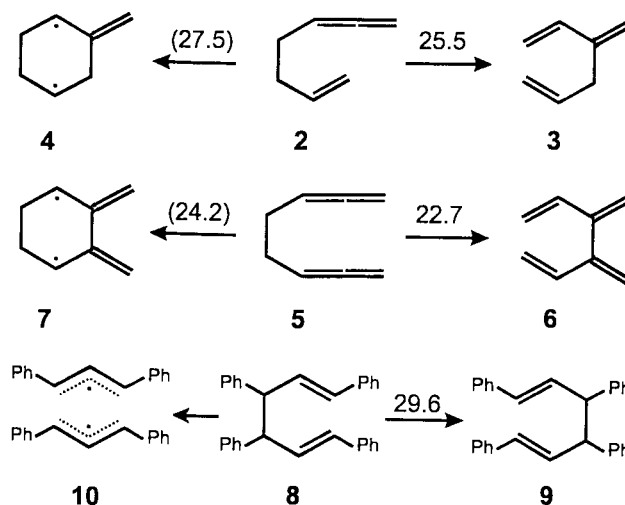
Scheme 2 Comparison between concerted and stepwise (in brackets) activation enthalpies[6,7] for the Cope rearrangement of hepta-1,2,6-triene (2), octa-1,2,6,7-tetraene (5), and 1,3,4,6-tetraphenylhexa-1,5-diene (8). All values in kcal mol^{-1}.

pathways: one leads to the diradical 4, the other bypasses 4 and leads directly to the product 3.[8] Recent ab initio and DFT calcu-lations have clarified this observation.[10]

In the case of 1,3,4,6-tetraphenylhexa-1,5-diene (8)[9] the path via two free allyl radicals (10) is not taken, instead the complex of the radical pair is formed. However, the concerted path is still more favourable[9] (Scheme 2).

Gas-phase studies by Roth et al.[11] on the thermolysis of 2,4-dimethylenetricyclo[3.3.0.0³,⁷]octane (o-stelladiene, 11), where the hexa-1,5-diene system is incorporated in a strained stellane skeleton, gave strong evidence that the rearrangement of 11 to tricyclo[5.2.1.0⁴,¹⁰]deca-1,6-diene (16) occurs via a

DOI: 10.1039/b000904k

J. Chem. Soc., Perkin Trans. 2, 2000, 1155–1163   **1155**

Table 1 Activation parameters for the rearrangements of **11** to **15** in d_8-toluene at 110 °C. The errors are statistical errors of regression analysis; the errors given in brackets [%] result from the analysis of kinetic errors using the formulae given by Heinzer and Oth [31]

|	**11**	**12**	**13**	**14**	**15**
$T/°C$	55–105	0–65	−20–32	50–105	50–105
$\log A$	13.63 ± 0.17 (0.9)	14.83 ± 0.06 (0.3)	15.21 ± 0.04 (0.3)	13.81 ± 0.09 (0.5)	13.18 ± 0.03 (0.2)
$E_a{}^a$	30.23 ± 0.27 (0.7)	26.99 ± 0.08 (0.3)	26.27 ± 0.05 (0.6)	31.45 ± 0.14 (0.3)	31.10 ± 0.05 (0.1)
$\Delta H^{\ddagger a}$	29.47 ± 0.27 (0.7)	26.22 ± 0.8 (0.4)	25.51 ± 0.05 (0.2)	30.68 ± 0.14 (0.4)	30.34 ± 0.05 (0.2)
$\Delta S^{\ddagger b}$	1.34 ± 0.77 (23.7)	6.84 ± 0.27 (15.2)	8.57 ± 0.18 (15.2)	2.17 ± 0.41 (13.5)	−0.71 ± 0.14 (15.3)
$\Delta G^{\ddagger a}$	28.96 (2.7)	23.60 (0.1)	22.22 (0.1)	29.85 (0.1)	30.61 (0.1)

^{a} kcal mol^{-1}. ^{b} cal mol^{-1} K^{-1}.

stepwise mechanism. This prompted us to investigate the thermolysis of **11** in solution and also to look at the thermolysis of related systems, with more and less strain energy. The examples which we studied were, besides **11**,[12] 4,6-dimethyl-enetricyclo[3.3.0.0^{3,7}]octan-2-one (**12**),[13] 2,4,6-trimethylene-tricyclo[3.3.0.0^{3,7}]octane (stellatriene, **13**),[15] 7,9-dimethylene-tricyclo[4.3.0.0^{3,8}]nonan-2-one (**14**),[14] and 2,7,9-trimethylene-tricyclo[4.3.0.0^{3,8}]nonane (**15**).[14]

Results

1. Thermolysis experiments

The syntheses of **11**–**15** have been described in the literature.[12–15] The thermolytic reactions of **11**–**15** were studied by measuring the concentrations of starting materials and products by means of ^{1}H NMR spectroscopy. The rearrangements of compounds **11**–**13** to the tricyclo[5.2.1.0^{4,10}]deca-1,6-diene derivatives **16**–**18**,[15] respectively, were found to follow first order kinetics. The same holds true for the twistbrendane species **14** and **15**, which rearrange upon heating to the tricyclo[6.2.1.0^{5,11}]undeca-1,7-diene derivatives **19** and **20**.[14] Both the starting materials and the products can be discriminated by their characteristic signals for the olefinic protons. The measurements were carried out at four to six different temperatures in the temperature range indicated in Scheme 3. At each temperature 20–30 measure-
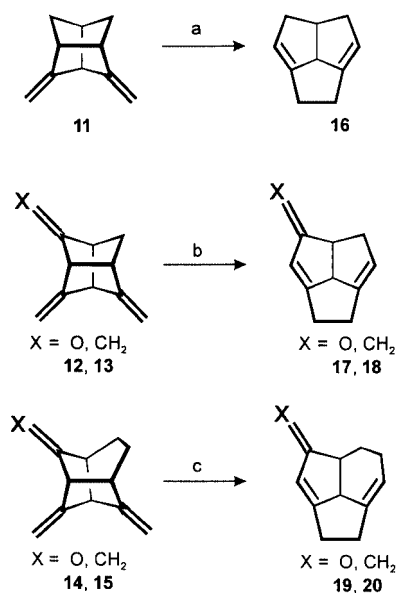
Scheme 3 Thermolysis reactions of **11**–**15** to yield **16**–**20**. **a**: 55–105 °C; **b**: **12**: 0–65 °C, **13**: −20–32 °C; **c**: 50–105 °C.

ments were taken. The solvent used was d_8-toluene. Specific rate constants are given in the Experimental section. The linear least-squares fit of the Arrhenius equation to the rate *vs.* temperature data (Fig. 1) afforded the parameters $\log A$ and E_a, from which the Eyring parameters were calculated for 110 °C (Table 1).

Table 2 Comparison of the activation parameters of **11** in d_8-toluene and in the gas-phase, as well as of **21** in the gas-phase at 110 °C

	11 (d_8-toluene)	**11** (gas-phase)[9]	**21** (gas-phase)[9]
$\log A$	13.63 ± 0.17	13.94 ± 0.24	13.97 ± 0.24
$E_a{}^a$	30.23 ± 0.27	31.4 ± 0.2	31.2 ± 0.4
$\Delta H^{\ddagger a}$	29.47 ± 0.27	30.6 ± 0.2	30.4 ± 0.2
$\Delta S^{\ddagger b}$	1.34 ± 0.77	2.74 ± 0.48	3.09 ± 1.14

^{a} kcal mol^{-1}. ^{b} cal mol^{-1} K^{-1}.
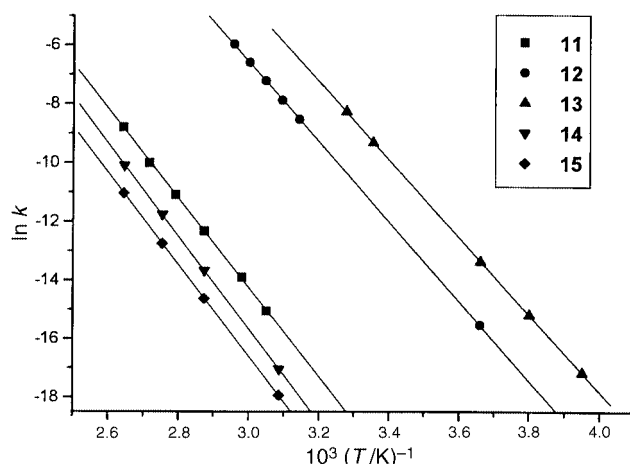
Fig. 1 Arrhenius plots for the Cope rearrangements of **11**–**15** in d_8-toluene.

Comments on the experimental results. The activation parameters measured for *o*-stelladiene **11** in d_8-toluene compare very well to those previously obtained in the gas-phase (Table 2).[11] This similarity suggests that the rearrangement of **11** follows the same mechanism in both the gas-phase and in solution. As has been deduced from the comparison to the ring opening reaction of the isomeric *p*-stelladiene **21**, the rearrangement of **11** is likely to occur *via* a two step mechanism.[11]
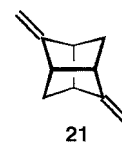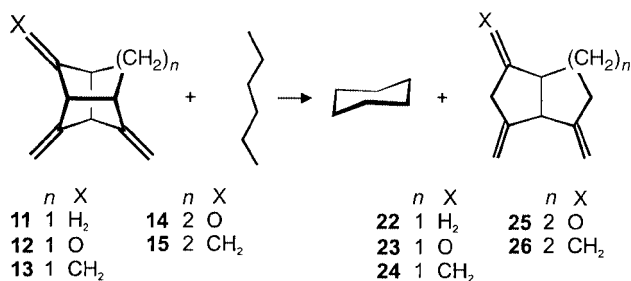
The strain energy inherent to these tricyclic molecules is crucial to the understanding of their reactivity. In Table 3 we give an overview of the strain energies (SE) for **11**–**15** obtained by force field calculations,[16] as well as values obtained from the homodesmotic reactions (ΔE) shown in Scheme 4. For these latter reactions it should be noted that the energy values obtained comprise only a part of the strain energy, the amount which is reduced in going from **11**–**15** to **22**–**26**, respectively.

As expected, the activation energies (E_a, Table 1) for the Cope rearrangement of **11**–**15** decrease with an increase of strain.

Table 3 Strain energies (SE) calculated for **11–15** with the MMX force field. Reduction of strain energy (ΔE, MP2/6-31G*//RHF/6-31G*) derived from the homodesmotic reactions of **11–15** shown in Scheme 4. All values in kcal mol^{-1}

	11	**12**	**13**	**14**	**15**
SE	58	62	66	50	54
ΔE	−32	−35	−35	−22	−22

n	X	n	X	n	X	n	X
11 1	H$_2$	**14** 2	O	**22** 1	H$_2$	**25** 2	O
12 1	O	**15** 2	CH$_2$	**23** 1	O	**26** 2	CH$_2$
13 1	CH$_2$			**24** 1	CH$_2$		

**Scheme 4** Homodesmotic reactions between **11–15** and hexane to **22–26**.

The measured values for the activation entropies ($\Delta S^{\ddagger}$) for **11–14** are positive. While for *o*-stelladiene **11** and the twistbrendanes **14** and **15** the activation entropy is very small (-1–2 cal mol^{-1} K^{-1}), one observes significantly positive values (7–9 cal mol^{-1} K^{-1}) for the stellane systems **12** and **13**. The positive values indicate an increase in mobility while the reaction proceeds from the highly rigid starting materials to the transition states. Significant positive $\Delta S^{\ddagger}$ values have also been reported for compounds in which terminal fluorine substituents strongly inhibit a pericyclic mechanism for a Cope rearrangement.[17]

2. Calculations

To learn more about the potential energy surfaces of the concerted and nonconcerted pathways for the [3,3]sigmatropic rearrangements of **11–15**, we carried out quantum chemical calculations. Extensive studies on the Cope rearragement of the parent system hexa-1,5-diene, have shown that it is necessary to use methods which can take into account the effects of both non-dynamic and dynamic electron correlation. On the basis of multireference-SCF (CASSCF) calculations followed by a perturbational correction of the CASSCF wave function (CASPT2 or MROPT2) it has been concluded that the prototype reaction follows a concerted pathway—in which bond making and bond breaking occur synchronously.[5]

The reactions presented here differ in two significant ways from the Cope rearrangement of hexa-1,5-diene. First, the polycyclic cage forces the hexa-1,5-diene system into the unfavourable boat conformation. Second, the strain energy inherent to these molecules destabilizes the breaking bond and makes a two step mechanism energetically competitive. Both effects in *o*-stelladiene **11** were studied in detail. Furthermore, the influence of conjugation was examined. While the additional double bond in stellatriene **13** might favour the two-step mechanism by further stabilizing the diradical intermediate, the enlarged bridge in 2,9-dimethylenetricyclo[4.3.0.0^{3,8}]nonane (twistbrendadiene, **27**) should favour the one-step pathway, by reducing the strain in the reactant. For **27** we have calculated the rearrangement to tricyclo[5.3.1.0^{4,11}]undeca-3,7-diene (**28**) (Scheme 5).

The crucial point in computational investigations of Cope rearrangements is the choice of an adequate theoretical method. As a rule of thumb one can state that methods which are based on a one determinant wave function tend to predict a one-step mechanism *via* an aromatic transition state. This applies to RHF, MP2 and DFT methods. On the other hand,
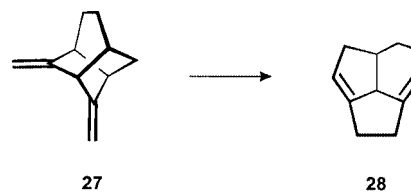
Scheme 5 Thermolysis of **27**.

methods which are based on a multiconfigurational wave function such as the CASSCF-procedure often overestimate the stability of diradicals and thus predict a two step mechanism.[18] Consequently, one has to choose a method which is able to describe closed-shell species and open-shell species in a balanced manner. The CASPT2 method developed by Roos *et al.*[19] is capable of doing so. Through a second order perturbational correction to the CASSCF wave function the effects of dynamical correlation are taken into account. Since this method does not allow the analytical computation of gradients, a geometry optimization is not feasible at this level of theory. To overcome these limitations we have chosen the following approach.

The closed-shell species, such as the reactants and the products as well as the transition state for the one-step mechanism ("aromatic" TS = TSAR), were optimized at the Hartree–Fock level. The open-shell species, the diradical intermediates and both the transition states TSE (from the starting material) and TSP (to the product) were optimized at the CASSCF level. The single point energy of all these six stationary points was then calculated using the CASPT2 method. Further insight into the nature of the CASPT2 surface was achieved by approximating the potential energy surface (PES) around these stationary points (TSE and TSAR) by means of a biquadratic function (CASPT2-2d-approximation).

2.1 Computational details. *Geometries.* The geometries of the starting materials **11**, **13**, **27**, the products **16**, **18**, **28**, and the corresponding "aromatic" (one-step) transition states TSAR-**11**, TSAR-**13**, and TSAR-**27** were optimized at the Restricted Hartree–Fock level (RHF) of theory. The geometries of the transition states describing a two-step mechanism, the TSE-**11**, TSE-**13**, TSE-**27**, TSP-**11**, TSP-**13**, TSP-**27**, as well as the diradical intermediates DIR-**11**, DIR-**13** and DIR-**27** (*cf.* Scheme 6) were optimized using the CASSCF-procedure.[20] Here, the active space of the CASSCF wave function includes six electrons distributed over six orbitals (CASSCF(6,6)). These orbitals correspond to each of the two π- and π^*-MOs and the σ/σ^*-MOs describing the breaking (C3–C4) bond. As it would appear that in the case of **13**, at least a CASSCF(8,8) should be necessary to give a correct description of the electronic structure, TSE-**13** has also been examined using the larger (8,8) active space. The CASSCF(6,6) and the CASSCF(8,8) geometries differ only by 0.75 kcal mol^{-1} in energy if one calculates the *single point* energy on the same (CASPT2(8,8)) level (*cf.* Table 4). The geometrical changes are minor, mainly concerning the bond length of one of the double bonds in the pentadienylic system. The CASSCF(6,6) wave function excludes one double bond from the active space, shortening its bond length from 1.35 to 1.32 Å.

Frequency calculations were carried out to characterize the nature of the stationary points and to obtain the thermodynamic data of interest. For the computation of the entropy and the thermodynamic correction to the enthalpy (ΔH) the unscaled frequencies were used ($T = 298.15$ K).

Single point energies. In order to obtain accurate values for the relative energy of all stationary points we performed single point CASPT2N calculations.[19] The active space of the corresponding CASSCF reference function varies, depending on the electronic structure and the number of double bonds. For the reactants and products, the active space includes only the

Table 4 Thermodynamic data for the Cope rearrangements of $11{\to}16$, $13{\to}18$ and $27{\to}28$. Entropy in cal mol^{-1} K^{-1}, ΔH and E_0^{CASPT2} in a.u. Single point: size of the active space for the single point CASPT2N calculation

Compound		Geom. opt.	v_{imag}	S	ΔH	Single point	E_0^{CASPT2}
11	C_s	RHF	—	89.1	0.214765	(4,4)	−386.919043
16	C_s	RHF	—	83.4	0.215911	(4,4)	−386.949813
DIR-**11**	C_1	CAS(6,6)	—	89.5	0.205948	(6,6)	−386.887578
TSAR-**11**	C_s	RHF	407 i	82.7	0.210439	(6,6)	−386.867714
TSE-**11**	C_s	CAS(6,6)	284 i	85.2	0.208082	(6,6)	−386.867213
TSP-**11**	C_s	CAS(6,6)	356 i	87.2	0.207314	(6,6)	−386.979277
13	C_2	RHF	—	85.3	0.220226	(6,6)	−424.833135
18	C_1	RHF	—	87.4	0.221869	(6,6)	−424.876875
DIR-**13**	C_1	CAS(6,6)	—	93.8	0.213087	(8,8)	−424.820767
TSAR-**13**	C_1	RHF	303 i	87.5	0.216250	(8,8)	−424.800311
TSE-**13**	C_1	CAS(6,6)	287 i	89.3	0.214160	(8,8)	−424.793389
	C_1	CAS(8,8)	a	—	—	(8,8)	−424.794587
TSP-**13**	C_1	CAS(6,6)	267 i	91.0	0.212896	(8,8)	−424.808029
27	C_1	RHF	—	85.7	0.247424	(4,4)	−426.116575
28	C_1	RHF	—	87.8	0.248195	(4,4)	−426.138708
DIR-**27**	C_1	CAS(6,6)	—	96.3	0.239407	(6,6)	−426.058487
TSAR-**27**	C_1	RHF	480 i	86.2	0.243049	(6,6)	−426.042089
TSE-**27**	C_1	CAS(6,6)	266 i	90.0	0.240069	(6,6)	−426.043629
TSP-**27**	C_1	CAS(6,6)	380 i	90.9	0.239271	(6,6)	−426.049749

a Too large for calculation.
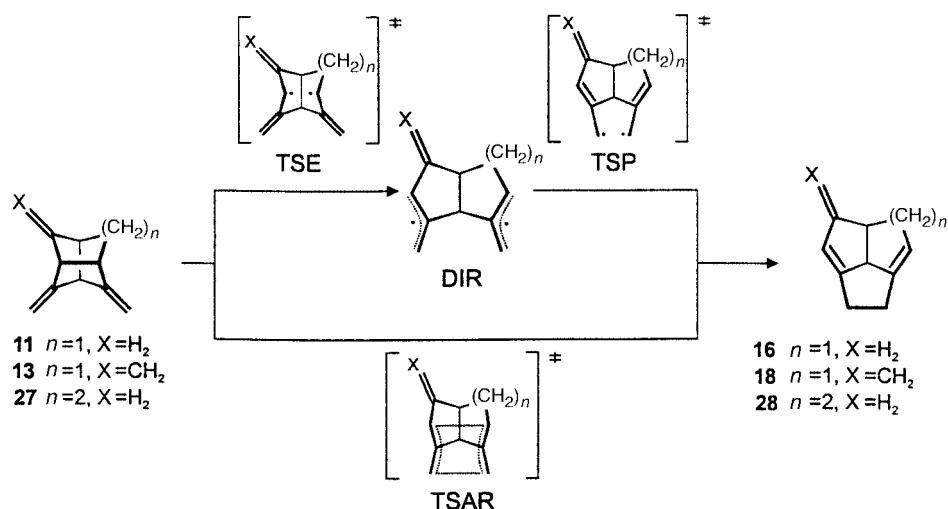
Scheme 6 Calculated routes for the one- and two-step mechanisms of the rearrangements of **11**, **13**, and **27** to **16**, **18**, and **28**, respectively. For the one-step mechanism the transition states are designated TSAR for the two-step mechanism TSE and TSP. The intermediates are designated DIR.

π- and π^*-MOs, thus resulting in a size of (4,4) for **11** or **27**, but (6,6) in the case of **13**. For the description of the "aromatic" transition states (TSAR), the diradicaloid transition states (TSE/TSP) and the diradical intermediates (DIR) the σ/σ^* orbitals of the breaking bonds and forming bonds must be taken into account. This allows for the correct electronic description of the allylic and pentadienylic moiety. The resulting sizes of the active spaces used for the computation of each species are given in Table 4.

Though it might seem disadvantageous to apply different active spaces for the same molecule, e.g. (4,4) for **11** but (6,6) for the transition state TSE-**11**, it has been shown earlier[20] that the CASPT2-energy of the species is not very sensitive to the size of the active space once all orbitals necessary for the description of the electronic structure have been taken into consideration.

The geometry optimizations and frequency calculations were carried out using the Gaussian 94[21] program. The CASSCF energies and the CASPT2N corrections to the energy were performed using the MOLCAS-3[22] and MOLCAS-4[23] program. The valence-double-ζ, polarized 6-31G* basis was used.[24]

CASPT2N-2d-approximation. As mentioned earlier, direct information about the CASPT2-PES is not available due to the lack of analytical gradients. We have chosen the following approach[25] to gain some insight into the behaviour on this level of theory. The CASPT2N-PES around the stationary points of interest, the TSE and the TSAR, was approximated by a biquadratic function of the type given in eqn. (1), where x

$$E(x,y) = E_0 + \tfrac{1}{2}k_x(x - x_0)^2 + \tfrac{1}{2}k_y(y - y_0)^2 + \tfrac{1}{2}k_{xy}(x - x_0)(y - y_0) \quad (1)$$

represents the length of the forming bond (C1–C6) and y represents the length of the breaking bond (C3–C4).[25] By determining five additional points $(x,y,E(x,y))$ around a stationary point, one can fit the biquadratic function to these six points. The resulting nonlinear set of equations can be solved iteratively to give the desired values for E_0, k_x, k_y, k_{xy}, x_0 and y_0. The biquadratic function—the approximated CASPT2-2d-PES—has a stationary point at (x_0,y_0) at an energy of E_0. The five additional points were obtained by arbitrarily choosing values for x and y in close proximity to the analytical stationary points. Next, restricted geometry optimizations with frozen values for x and y were carried out, leading to $E(x,y)$ (RHF for the TSARs and CASSCF(6,6) for the TSEs). At first, the RHF (CASSCF, resp.) energies ($E(x,y)$ in eqn. (1)) were obtained in order to prove that these points were well chosen. In all cases, eqn. (1) exhibits a saddle point, the energy of which is equal ($|E_0 - E_{exact}| < 1.1$ kcal mol^{-1}) to the analytical one, and the
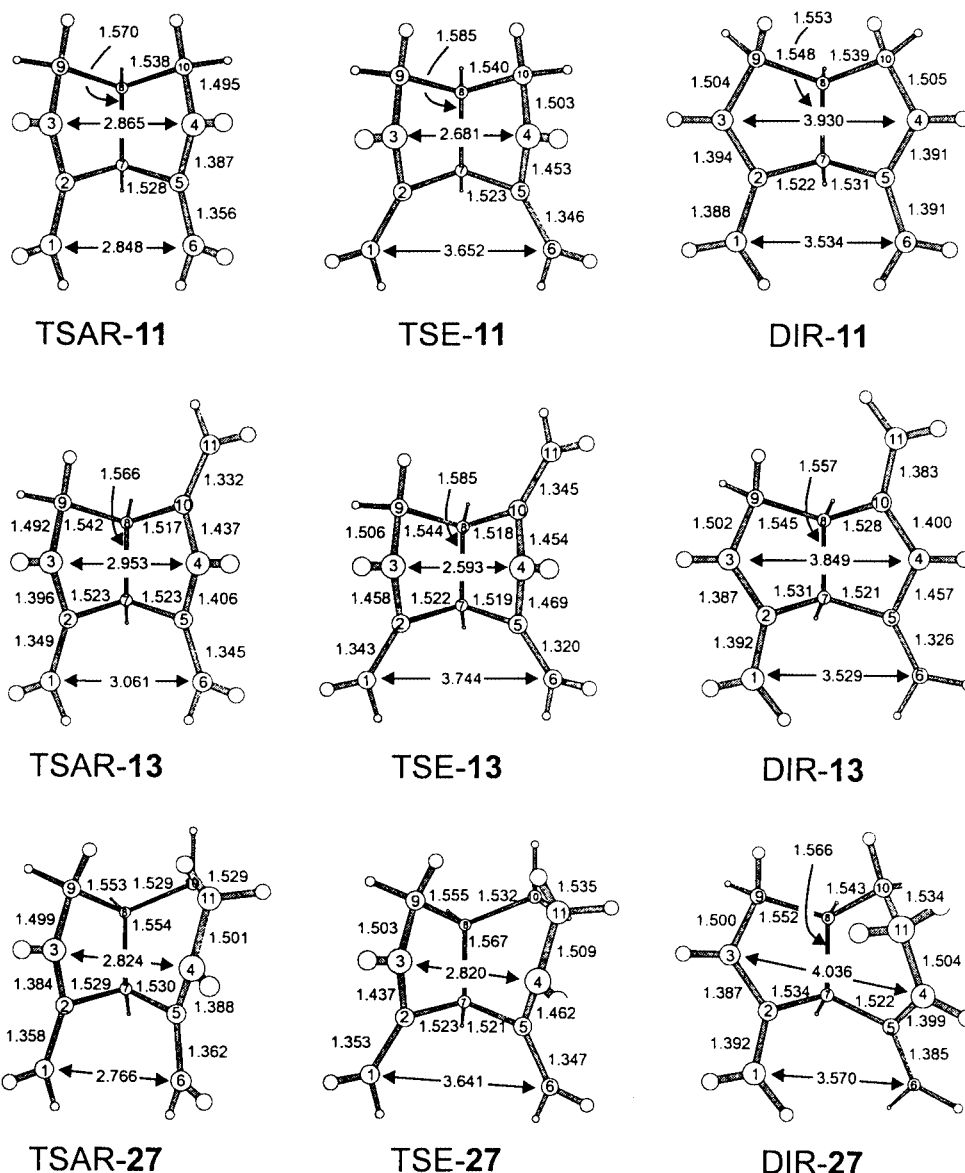
Fig. 2 Most relevant distances (Å) calculated for the transition states TSAR, TSE, and the intermediates DIR of the rearrangements of **11**, **13** and **27**.

geometrical distance[26] is within a range of 0.03 Å. Using the same (x,y)-values, the single point energy $E(x,y)$ was then calculated at the CASPT2N level of theory. Solving the new set of equations resulted in an approximation of the CASPT2N-PES in the region around the stationary points.

2.2 Results. *Cope rearrangement of 11 to 16.* Parts of the results have already been published elsewhere[11] (see also Table 4 and Fig. 2). On the RHF-PES of **11** a total of three stationary points have been found: the reactant **11**, the product **13** and the TSAR-**11**. The most striking feature of *o*-stelladiene **11** is the elongated breaking bond, C3–C4 = 1.608 Å. This must be attributed to the high strain energy present in this class of molecules, which is also the driving force for the Cope rearrangement. The distance between the double bond termini is 4.059 Å. The TSAR-**11** shows a very large separation of the two allylic moieties. Their distance, 2.8 Å, is markedly larger than reported for the boat-TS of hexa-1,5-diene (2.20 Å).[4h] Furthermore, this value is outside the range expected for a partial single bond.[27] This indicates that there is no possibility for aromatic stabilization to take place.

On the CASSCF(6,6)-PES a total of four stationary points has been found. Two of them, the TSE-**11** and the DIR-**11** (C_s) have been discussed in detail elsewhere.[11] The DIR-**11** (C_s) is

not a true minimum, but a first order saddle point connecting the two enantiomeric DIR-**11** (C_1). While both the C_s and C_1 symmetric species are very close in energy ($\Delta E = 1.95$ kcal mol^{-1}), they differ significantly in their entropy, thus changing the activation parameters for the reaction of DIR-**11** to **11** and DIR-**11** to **16**. The diradical DIR-**11** (C_1) profits from the loss of strain energy, which leads to a very open structure with a distance between the allylic moieties of more than 3.5 Å. It is noteworthy that the TSAR-**11** vanishes on the CASSCF(6,6) PES. All attempts to localize a minimum or a transition state starting at the TSAR-**11** geometry lead either to the DIR-**11** or the TSE-**11**.

The CASPT2N-2d approximation shows, that the TSE-**11** is likely to remain unchanged on the CASPT2N level of theory. The saddle point of the approximated PES is very close in energy ($\Delta E = -1.9$ kcal mol^{-1}) to the one found analytically on the CASSCF surface. The C3–C4 distance enlarges from 2.68 Å (TSE-**11**) to 2.86 Å (y_0-TSE-**11**) whereas the C1–C6 distance shortens from 3.65 Å to 3.41 Å (x_0-TSE-**11**). This suggests a more compact geometry on the CASPT2 level, in accordance with the behaviour found for the Cope rearrangement of hexa-1,5-diene.[5] For the TSAR-**11** no stationary point could be detected in the vicinity of the analytical RHF-TSAR-**11**. Depending on the choice of the $(x,y,E(x,y))$ triples one finds
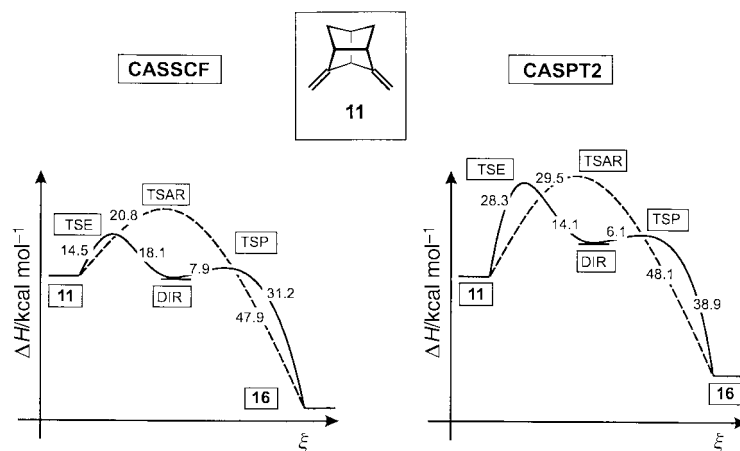
Fig. 3 Calculated reaction profiles for a one- and two-step rearrangement of **11** to **16** by using the CASSCF (left) and CASPT2 approach.

Table 5 Diradical character (DR = 2 − n(HOMO) of the natural orbital CASSCF wave function) for the stationary points of the Cope rearrangement of **11→16**, **13→18** and **27→28**

	Reactant	TSE	TSAR	DIR	TSP	Product
11→16	0.07	0.39	0.46	0.89	0.49	0.07
13→18	0.08	0.33	0.56	0.93	0.54	0.10
27→28	0.08	0.48	0.43	0.96	0.57	0.08

saddle points or minima in the range of $\Delta r > 2$ Å and $\Delta E > 10$ kcal. This indicates that the CASPT2-PES is not sufficiently parallel to the RHF-PES in this region. We conclude, that there is no "aromatic" transition state in the proximity of the TSAR-**11** on the CASPT2 PES.

The PES of the Cope rearrangement of *o*-stelladiene **11** is very flat in the region of interest, between the TSAR-**11** and TSE-**11**. Dupuis, Murray and Davidson have argued that in such cases the CASSCF method might lead to computational artifacts.[4g] Nevertheless, the CASPT2N-2d approximation demonstrates that the CASSCF-optimized TSE-**11** remains a transition state even on the CASPT2-2d level. The geometries of the transition states are strongly influenced by the rigid carbon-skeleton; therefore, large changes in the geometry do not occur on going from CASSCF to CASPT2N-2d.

However, comparison of the CASSCF and CASPT2 reaction profiles for the Cope rearrangement of *o*-stelladiene **11** (Fig. 3) shows the importance of including dynamic correlation on energetics. Based on the CASSCF energy profile, DIR-**11** should be even more stable than the reactant *o*-stelladiene **11**. As a result of this energetic preference for the diradical intermediate, the activation energy is predicted to be 15 kcal mol⁻¹ too low. This deficiency is overcome by the CASPT2 method, which raises the energy of the diradical DIR-**11** relative to the reactant.

Cope rearrangement of 13 to 18. The overall effect of the double bond is reflected in the lowering of the activation energy by approximately 10 kcal mol⁻¹ for both alternative pathways (Fig. 4, left). Compared to the *o*-stelladiene system, the distance between the allylic moieties is about 0.1 Å larger for the TSAR-**13**. But for the two-step pathway instead, the bond breaking process occurs at a shorter C3–C4 distance, 2.59 Å in TSE-**13** compared to 2.68 Å for TSE-**11**. This indicates that the TSE-**13** is "earlier" on the reaction coordinate, in good agreement with the energetics of the reaction: the stabilization of the intermediate by the double bond causes the reactant **13** and the diradical DIR-**13** to be nearly equal in energy.

The results of the CASPT2N-2d approximation are noteworthy. For the TSE-**13** a behaviour similar to the TSE-**11** is observed. Again the TSE-**13** is predicted to have a more compact geometry on the CASPT2N level ($x_0 = 3.53$ Å, $y_0 = 2.52$ Å)

compared to the CASSCF geometry (C1–C6 and C3–C4 in Fig. 1), but the associated change in energy is minor ($\Delta E = -0.3$ kcal mol⁻¹).

In the case of the TSAR-**13**, the approximation of the PES leads to a saddle point with a very large distance between the double bond termini ($x_0 = 4.44$ Å, $y_0 = 3.09$ Å) but only 1.8 kcal mol⁻¹ lower in energy than the analytical one. The very flat PES between the TSAR-**13** and the TSE-**13** does not allow us to decide whether the TSAR-**13** vanishes on the CASPT2 surface or not. Since the one-step pathway is energetically preferred, it must be considered to be the predominant pathway.

The influence of the double bond is unexpected. From chemical intuition one might have expected, that the reaction path *via* the diradical should be favoured through the effect of conjugation. A comparison of the diradical character (DR = 2 − n(HOMO), *cf.* Table 5) of the "non-stabilized" species in the *o*-stelladiene system brings clarification. In this case the diradical character DR approaches the value of 1.0 which indicates a "perfect" diradical. A comparison of the calculated activation parameters with experiment yields good agreement in the case of **11** ($\Delta H_{exp} = 29.5$ kcal mol⁻¹, $\Delta H_{calc} = 29.0$ kcal mol⁻¹) while the agreement in the case of **13** ($\Delta H_{exp} = 25.5$ kcal mol⁻¹, $\Delta H_{calc} = 21.0$ kcal mol⁻¹) is less good, but within the expectation.

Remarkably, the TSAR-**11** has a slightly higher diradical character (0.46) than the TSE-**11** (0.39). Thus, the former should benefit more from conjugation with the double bond.

Cope rearrangement of 27 to 28. The most significant difference between the twistbrendane and the stellane system can be found in their strain energy. From the force field and *ab-initio* calculations (see Table 3) this difference can be estimated to be approx. 10 kcal mol⁻¹, the twistbrendane system being less strained. This is reflected in the higher activation energy for the Cope rearrangement of twistbrendadiene **27** (Fig. 4, right). Additionally, the C3–C4-bond length in **27** (1.586 Å) is distinctly shorter than in *o*-stelladiene **11**.

The CASPT2N-2d approximation for the TSE-**27** shows that this saddle point prevails on the CASPT2 surface, again with a tighter geometry ($x_0 = 3.32$ Å, $y_0 = 2.76$ Å, $\Delta E = -0.8$ kcal mol⁻¹).

The CASPT2N-2d approximation of the TSAR-**27** results in a minimum, geometrically in between the TSE-**27** and the DIR-**27**. This indicates that the TSAR-**27** is not a stationary point on the CASPT2 surface but belongs to the "valley" of the diradical DIR-**27**, contrary to chemical intuition. The loss of strain energy does not allow for the one step mechanism to become the preferred one. Instead, the reaction proceeds *via* the two-step mechanism. The TSE-**27** is now "late" on the reaction coordinate compared to TSE-**11**, as can be concluded by the length of the breaking bond and the diradical character.
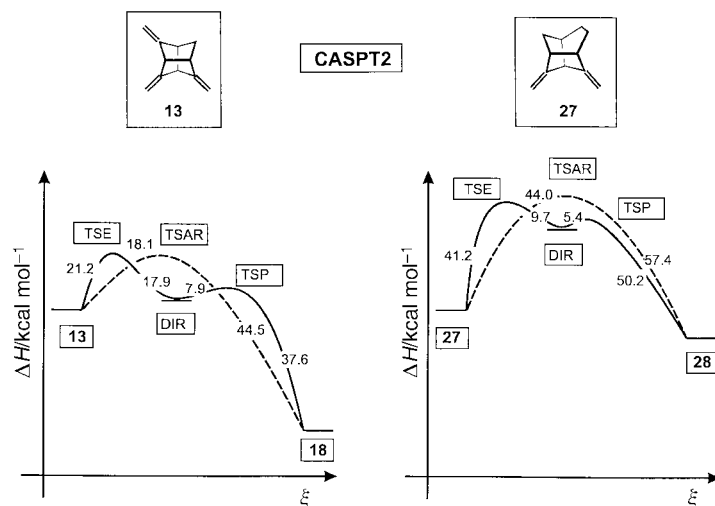
Fig. 4 Calculated reaction profiles (CASPT2) for a one- and two-step mechanism for the rearrangement of **13** to **18** (left) and **27** to **28** (right).
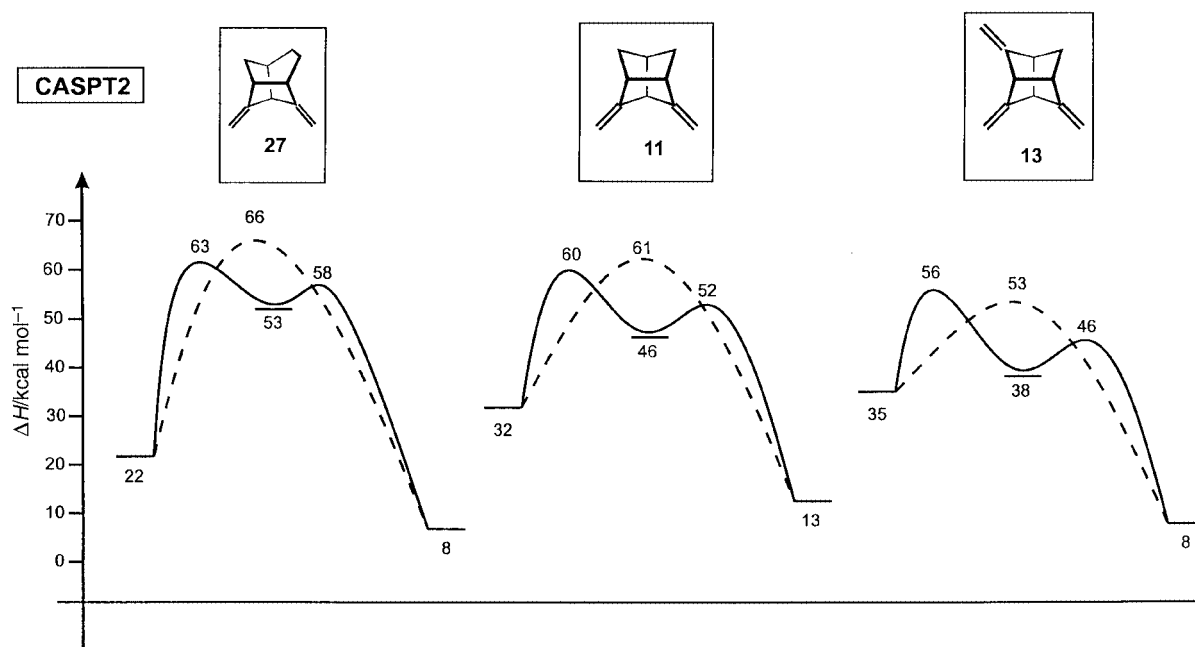

Fig. 5 Comparison of the reaction profiles of the Cope rearrangements of **11** (center), **13** (right) and **27** (left) in consideration of the strain energy.

## Comparison of the calculated activation energies for 11, 13 and 27

For a comparison of the calculations for **11**, **13** and **27** it is reasonable to use a common starting point. In Fig. 5 we have chosen the energy of the starting material, corrected by the calculated release of strain energy. This seems reasonable if the bond-breaking step is rate determining.

The activation energies for the one step-mechanism *via* TSE-**11** and TSE-**27** amount to approx. 60 kcal mol^{-1}, taking the hypothetical unstrained systems as a reference. Interestingly, this is close to the energy of two allyl radicals (55.7 kcal mol^{-1}).[5a]

The introduction of a "vinyl-group" in the "3"-position of the hexa-1,5-diene system as in stellatriene **13**, leads to a lowering of the activation-barrier for the two-step mechanism by 4 kcal mol^{-1}. For the one-step-mechanism *via* TSAR-**13**, a stabilization twice as large is observed (8 kcal mol^{-1}). Interestingly, this is the same amount by which the DIR-**11** is stabilized relative to the diradical DIR-**13**. As a consequence, the "aromatic" transition state should no longer be pronounced as aromatic, since there is no evidence for aromatic stabilization whatsoever. Instead, the TSARs might be regarded as two allyl radicals held in close proximity by the carbon skeleton, allowing for a weak

interaction. This pathway would be somewhere in between (a) and (b) in Scheme 1.

Comparison of the first step of the Cope rearrangement of **11** and **27** shows that the higher activation energy of **27** can mainly be attributed to the difference in strain energy between the stellane and twistbrendane system: the TSE-**27** and the TSE-**11** show only a minor difference if compared on the "absolute" scale in Fig. 5. The remaining energy-difference of 3 kcal mol^{-1} can be explained by the different conformations observed for the five- and six-membered rings, as shown in structures **29** and **30**. Whereas the cyclopentane-ring can achieve its preferred envelope-conformation, the cyclohexane-

29   **30**
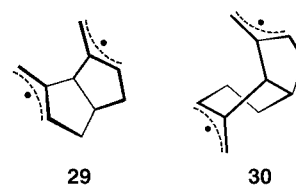
ring in **27** is forced into the unfavourable twisted conformation. This effect is even more important for the intermediates and the TSARs.

Discussion

The model calculations for the rearrangements of **11** to **16**, **13** to **18**, and **27** to **28** reveal only small energy differences between a stepwise and concerted mechanism. The results of the calculations favour a stepwise mechanism for the Cope rearrangement of **11** and **27** while for **13** a concerted path should be slightly favoured.

Arguments from experiment for a stepwise mechanism are due to the investigations of **11** and **21** in the gas-phase.[11] All the evidence in these investigations (trapping of intermediates with O_2) and similarity of kinetic data between **11** and **21** support the formation of a diradical intermediate. By the same token we interpret the similarity of the kinetic data obtained for **11** in solution and in the gas-phase that the rate determining step is the bond cleavage of one of the central C–C σ-bonds of the stellane skeleton.

Geometric inspection provides further support. The terminal methylene groups in derivatives of **11**–**13** are found to be separated by more than 4 Å.[28] To assist the breaking of the central C–C σ-bond in **11**–**13**, *i.e.* to support the concerted pathway, the terminal CH_2 groups would have to approach each other within *ca.* 3 Å. According to force field calculations this would require about 15 to 16 kcal mol^{-1}.[11] This value is too large for its loss to be compensated by the energy gained in the concerted reaction. A further argument is the weakening of the bonds between the bridgehead atoms in the tricyclo[3.3.0.0[3,7]]octane skeleton of **11**–**13**. X-Ray investigations on derivatives reveal bond lengths in the order of 1.61 to 1.62 Å.[28] In the case of derivatives with the twistbrendane skeleton the bond lengths between the bridgehead positions amount to 1.58 Å.[29] A third argument which supports the stepwise mechanism is the observation that the replacement of all the terminal CH_2 groups in **13** by isopropylidene groups leads only to a very moderate stabilization.[15]

An argument in favour of a stepwise Cope rearrangement in the case of **11** to **16** are the successful trapping experiments. To explore the possibilities of diradical intermediates further we have carried out the thermolyses of **11**, **12**, and **15** in the presence of cyclohexa-1,4-diene. In the case of **12** we were able to detect masses (GCMS) of the 1 : 1 products with cyclohexa-1,4-diene and also the dihydrogenated species of **12**. A similar experiment with **11** and CCl_4 revealed (GCMS) a 1 : 1 adduct when heated to 74 °C.

Conclusion

We provide in this paper experimental and theoretical investigations on a series of compounds in which a hexa-1,5-diene unit is fixed in such a way that a delocalization in the transition state of the Cope rearrangement is difficult to achieve. The experimentally determined activation energies in the series **11**–**15** parallel approximately those of the calculated strain energies. However, the results of the calculations show that in all cases studied, the difference in activation energy between a stepwise or concerted mechanism should be small. Noteworthy is the result that a reduction of strain energy (**11**→**27**) does not favour the concerted pathway. The increase of conjugation in the transition state in going from **11** to **13** lowers the energy of both pathways, the concerted and the stepwise one. Further experimental effort will provide a better understanding of the Cope rearrangement in rigid systems. Preliminary calculations[30] show that secondary kinetic isotope effects (SKIE) should allow discrimination between a stepwise or concerted reaction path.

Experimental

The preparation of the starting materials **11**–**15** have been described in the literature.[11–13] The analytical data of the corre-

sponding products **17** and **18**[14] as well as **19** and **20**[13] appear in the literature. The NMR data of **16** are as follows: ^{1}H NMR (200 MHz, d_8-toluene): δ 5.09–5.08 (m, 2H); 3.65–3.58 (m, 1H); 3.14–3.00 (dd, 2H, [2]J = 15.5 Hz, [3]J = 8.6 Hz); 2.80–2.66 (m, 1H); 2.48–2.25 (m, 4H); 2.21–2.09 (d, 2H, [2]J = *ca.* 16 Hz); ^{13}C NMR (50.32 MHz, d_8-toluene): δ 150.96 (s), 121.67 (d, 2C), 69.26 (d), 48.62 (t, 2C), 37.88 (d), 30.40 (t, 2C).

The thermolysis reactions were carried out in quartz NMR tubes. For this purpose we dissolved 15–20 mg of the sample in 0.5 ml of the solvent under an argon atmosphere. In the case of **12** and **13** the solution was prepared at −30 °C, the other samples were dissolved at room temperature. Traces of oxygen were removed by the freeze-pump-thaw technique. All operations were carried out under an argon atmosphere. The temperature could be kept constant to within ±0.1 °C. The reaction was followed by ^{1}H NMR spectroscopy (200 MHz) by measuring the ratio of the olefinic protons of the starting material and of the product. For each temperature 20–30 NMR spectra were taken. By assuming a first order rate law the rate constant could be determined from the concentration of the starting material (C_{Ao}) at t_o and the concentration C_A at time t using eqn. (2).

$$\ln \frac{C_A}{C_{Ao}} = k\,(t - t_o) \qquad (2)$$

Specific rate constants are given in Table 6. To derive E_a and ln A the rate constants were regressed by linear least squares fitting to the Arrhenius equation. The correlation coefficient r^2 was in all cases greater than 0.9996. To calculate $\Delta H^{\ddagger}$ and $\Delta G^{\ddagger}$ we used the Eyring equation. The errors given in Table 1 are statistical errors that result from the regression analysis of the Arrhenius plot. In addition the kinetic errors were analyzed using the formulae given by Heinzer and Oth.[31] This error treatment is based on the errors in k and T at the highest and lowest temperature employed for the measurements.

Trapping experiments

20 mg of **11** (6 h at 105 °C), **12** (24 h at 20 °C), and **15** (72 h at 90 °C) were heated in sealed ampoules in an excess of cyclohexa-1,4-diene. The reaction mixture was analyzed by GCMS (Hewlett Packard HP 5972 GC/MS-MSD-Workstation). Only in the case of **12** (m/z = 146) were masses corresponding to trapping products found. Four products of mass m/z = 226 (1 : 1 adduct with cyclohexa-1,4-diene) and one product of mass m/z = 148 (addition of two hydrogen atoms) were detected. In similar experiments with **21** no trapping products were detected.[32]

GCMS (EI, 70 eV) data of the trapping products of 12.[33] *1 : 1 adducts:*
a) m/z (%): 226 (0.3), 211 (0.3), 198 (65), 183 (7), 170 (39), 144 (39), 143 (29), 129 (58), 128 (33), 118 (51), 117 (84), 116 (30), 115 (44), 107 (23), 106 (36), 105 (41), 104 (30), 103 (20), 92 (34), 91 (100), 79 (74), 78 (39), 77 (80), 65 (26), 51 (21).
b) m/z (%): 226 (6), 147 (100), 117 (35), 91 (41), 79 (38), 77 (40).
c) m/z (%): 226 (13), 211 (3), 198 (10), 183 (4), 148 (23), 147 (100), 129 (20), 119 (23), 118 (39), 117 (73), 115 (29), 105 (23), 91 (93), 73 (65), 78 (29), 77 (71), 65 (20).
d) m/z (%): 226 (0.2), 198 (0.2), 183 (0.2), 147 (100).
e) 2H adduct: m/z (%): 148 (44), 147 (20), 133 (56), 105 (100), 103 (31), 79 (60), 77 (60), 66 (69), 51 (20).

Additionally 15 mg (0.11 mmol) of **11** in 1 ml of CCl_4 was heated in a sealed ampoule for 10 days at 74 °C. The mixture was analyzed by GCMS and contained a product of mass m/z = 284. This value and the isotopic distribution is in agreement with a 1 : 1 product between **11** and CCl_4.

Table 6 Experimental rate constants for the Cope rearrangements of **11**–**15** in d_8-toluene

11		12		13		14		15	
T/°C	k/s^{-1}	T/°C	k/s^{-1}	T/°C	k/s^{-1}	T/°C	k/s^{-1}	T/°C	k/s^{-1}
54.6	2.84×10^{-7}	0.0	1.76×10^{-7}	-20.0	3.48×10^{-8}	50.9	3.93×10^{-8}	50.9	1.61×10^{-8}
62.3	9.09×10^{-7}	45.0	1.94×10^{-4}	-10.0	2.54×10^{-7}	74.9	1.15×10^{-6}	74.9	4.42×10^{-7}
74.8	4.38×10^{-6}	50.0	3.73×10^{-4}	0.0	1.56×10^{-6}	90.0	7.79×10^{-6}	90.0	2.90×10^{-6}
84.9	1.50×10^{-5}	55.0	7.22×10^{-4}	25.0	9.04×10^{-5}	104.8	4.10×10^{-5}	105.0	1.61×10^{-5}
94.8	4.47×10^{-5}	60.0	1.36×10^{-3}	32.0	2.57×10^{-4}				
105.1	1.50×10^{-4}	65.0	2.55×10^{-3}						

GCMS (70 eV, EI) data of the trapping product of 11.[33] m/z (%) 288 (11), 286 (24), 284 (19), 251 (17), 249 (18), 177 (41), 167 (51), 151 (38), 142 (25), 141 (31), 131 (100), 128 (21), 127 (21), 125 (36), 116 (23), 115 (58), 91 (56), 79 (36), 77 (46), 51 (21).

Acknowledgements

References

1 A. C. Cope and E. M. Hardy, *J. Am. Chem. Soc.*, 1940, **62**, 441.
2 (*a*) W. v. E. Doering and W. R. Roth, *Tetrahedron*, 1962, **18**, 67; (*b*) H. E. Zimmerman, *J. Am. Chem. Soc.*, 1966, **88**, 1564; (*c*) H. M. Frey and R. Walsh, *Chem. Rev.*, 1969, **69**, 103; (*d*) W. v. E. Doering, V. G. Toscano and G. H. Beasley, *Tetrahedron*, 1971, **27**, 5299; (*e*) S. J. Rhoads and N. R. Raulins, *Org. React. NY*, 1975, **22**, 1; (*f*) R. Wehrli, H. Schmid, D. Belluš and H.-J. Hansen, *Helv. Chim. Acta*, 1977, **60**, 1325; (*g*) M. J. S. Dewar and L. E. Wade, *J. Am. Chem. Soc.*, 1973, **95**, 290; M. J. S. Dewar and L. E. Wade, *J. Am. Chem. Soc.*, 1977, **99**, 4417; (*h*) W. v. E. Doering, *Proc. Natl. Acad. Sci. USA*, 1981, **78**, 5279; (*i*) J. J. Gajewski, *Acc. Chem. Res.*, 1980, **13**, 142.
3 (*a*) M. J. S. Dewar, G. P. Ford, M. L. McKee, H. S. Rzepa and L. E. Wade, *J. Am. Chem. Soc.*, 1977, **99**, 5069; (*b*) M. J. S. Dewar and E. R. Healy, *J. Phys. Lett.*, 1987, **141**, 521; (*c*) M. J. S. Dewar and C. Jie, *J. Am. Chem. Soc.*, 1987, **109**, 5893; (*d*) M. J. S. Dewar and C. Jie, *J. Chem. Soc, Chem. Commun.*, 1987, 1451; (*e*) M. J. S. Dewar and C. Jie, *J. Chem. Soc., Chem. Commun.*, 1989, 98; (*f*) M. J. S. Dewar and C. Jie, *Acc. Chem. Res.*, 1992, **25**, 537.
4 (*a*) A. Komornicki and J. W. McIver, *J. Am. Chem. Soc.*, 1976, **98**, 4553; (*b*) Y. Osamura, S. Kato, K. Morokuma, D. Feller, E. R. Davidson and W. T. Borden, *J. Am. Chem. Soc.*, 1984, **106**, 3362; (*c*) K. Morokuma, W. T. Borden and D. A. Hrovat, *J. Am. Chem. Soc.*, 1988, **110**, 4474; (*d*) W. T. Borden, R. J. Loncharich and K. N. Houk, *Annu. Rev. Phys. Chem.*, 1998, **39**, 213; (*e*) M. Bearpark, F. Bernardi, M. Olivucci and M. A. Robb, *J. Am. Chem. Soc.*, 1990, **112**, 1732; (*f*) W. T. Borden, D. A. Hrovat, R. L. Vance, N. G. Rondan, K. N. Houk and K. Morokuma, *J. Am. Chem. Soc.*, 1990, **112**, 2018; (*g*) M. Dupuis, C. Murray and E. R. Davidson, *J. Am. Chem. Soc.*, 1991, **113**, 9756; (*h*) H. Jiao and P. v. R. Schleyer, *Angew. Chem.*, 1995, **107**, 329; H. Jiao and P. v. R. Schleyer, *Angew. Chem., Int. Ed. Engl.*, 1995, **34**, 334; (*i*) K. N. Houk, J. Gonzalez and Y. Li, *Acc. Chem. Res.*, 1995, **28**, 81.
5 (*a*) D. A. Hrovat, K. Morokuma and W. T. Borden, *J. Am. Chem. Soc.*, 1994, **116**, 1072; (*b*) R. M. Kozlowski, M. Dupuis and E. R. Davidson, *J. Am. Chem. Soc.*, 1995, **117**, 774.
6 J. J. Gajewski and N. D. Conrad, *J. Am. Chem. Soc.*, 1979, **101**, 6693.
7 K. Humski, R. Malojčić, S. Borčić and D. E. Sunko, *J. Am. Chem. Soc.*, 1970, **92**, 6534.
8 W. R. Roth, D. Wollweber, R. Offerhaus, V. Rekowski, H.-W. Lennartz, R. Sustmann and W. Müller, *Chem. Ber.*, 1993, **126**, 2701.
9 W. R. Roth and F. Hunold, *Liebigs Ann.*, 1996, 1917.
10 D. A. Hrovat, J. A. Duncan and W. T. Borden, *J. Am. Chem. Soc.*, 1999, **121**, 169.
11 W. R. Roth, R. Gleiter, V. Paschmann, U. E. Hackler, G. Fritzsche and H. Lange, *Eur. J. Org. Chem.*, 1998, 961.
12 R. Gleiter and B. Kissler, *Tetrahedron Lett.*, 1987, **28**, 6151.
13 R. Gleiter, C. Sigwart and B. Kissler, *Angew. Chem.*, 1989, **101**, 1561; R. Gleiter, C. Sigwart and B. Kissler, *Angew. Chem., Int. Ed. Engl.*, 1989, **28**, 1525.
14 R. Gleiter, T. Herb, O. Borzyk and I. Hyla-Kryspin, *Liebigs Ann. Chem.*, 1995, 357.
15 R. Gleiter and C. Sigwart, *J. Org. Chem.*, 1994, **59**, 1027.
16 W. Burkert and N. L. Allinger, *Molecular Mechanics*, ACS Monograph 1982, 177; J. J. Gajewski and K. F. Gilbert, MMX: Consistent of Rotines MM2 + MMPI, Serena Software, Bloomington, IN, USA.
17 W. R. Dolbier, Jr. and K. W. Palmer, *J. Am. Chem. Soc.*, 1993, **115**, 9349.
18 K. A. Black, S. Wilsey and K. N. Houk, *J. Am. Chem. Soc.*, 1998, **20**, 5622.
19 K. Andersson, P.-A. Malmquist, B. O. Roos, A. Sadlej and K. Wokinski, *J. Phys. Chem.*, 1990, **94**, 5483; K. Andersson, P.-A. Malmquist and B. O. Roos, *J. Chem. Phys.*, 1992, **96**, 1218.
20 (*a*) P. E. M. Siegbahn, J. Almlöf, A. Heiberg and B. O. Roos, *J. Chem. Phys.*, 1981, **74**, 2384; (*b*) R. Shepard, *Adv. Chem. Phys.*, 1987, **69**, 63; (*c*) B. O. Roos, in *Ab Initio Methods in Quantum Chemistry - II*, ed. K. P. Lawley, John Wiley & Sons, 1987, p. 399.
21 Gaussian 94, Revision D.2, M. J. Frisch, G. W. Trucks, H. B. Schlegel, P. M. W. Gill, B. G. Johnson, M. A. Robb, J. R. Cheeseman, T. Keith, G. A. Petersson, J. A. Montgomery, K. Raghavachari, M. A. Al-Laham, V. G. Zakrzewski, J. V. Ortiz, J. B. Foresman, J. Cioslowski, B. B. Stefanov, A. Nanayakkara, M. Challacombe, C. Y. Peng, P. Y. Ayala, W. Chen, M. W. Wong, J. L. Andres, E. S. Replogle, R. Gomperts, R. L. Martin, D. J. Fox, J. S. Binkley, D. J. Defrees, J. Baker, J. J. P. Stewart, M. Head-Gordon, C. Gonzalez and J. A. Pople, Gaussian, Inc., Pittsburgh PA, 1995.
22 MOLCAS Version 3, K. Andersson, M. R. A. Blomberg, M. P. Fülscher, V. Kellö, R. Lindh, P.-Å. Malmqvist, J. Noga, J. Olsen, B. O. Roos, A. J. Sadlej, P. E. M. Siegbahn, M. Urban and P.-O. Widmark, University of Lund, Sweden, 1994.
23 MOLCAS Version 4. K. Andersson, M. R. A. Blomberg, M. P. Fülscher, G. Karlström, R. Lindh, P.-Å. Malmqvist, P. Neogrady, J. Olsen, B. O. Roos, A. J. Sadlej, M. Schütz, L. Seijo, L. Serrano-Andres, P. E. M. Siegbahn and P.-O. Widmark, University of Lund, Sweden, 1997.
24 P. C. Hariaharan and J. A. Pople, *Theor. Chim. Acta*, 1973, **28**, 213.
25 W. T. Borden, personal communication.
26 sqrt $((R(C1-C6) - x_0)^2 + (R(C3-C4) - y_0)^2)$.
27 K. N. Houk, Y. Li and J. D. Evanseck, *Angew. Chem.*, 1992, **104**, 711.
28 V. Siemund, H. Irngartinger, C. Sigwart, B. Kissler and R. Gleiter, *Acta Crystallogr.*, *Sect. C*, 1993, **49**, 57.
29 O. Borzyk, Dissertation, Universität Heidelberg, 1994.
30 H. Lange, Dissertation, Universität Heidelberg, 1998; W. T. Borden, unpublished results.
31 J. Heinzer and J. F. M. Oth, *Helv. Chim. Acta*, 1981, **64**, 258.
32 B. Gaa, Diplomarbeit, Universität Heidelberg, 1996.
33 Only those peaks with $m/z > 50$ were listed. Non-characteristic peaks with relative intensities $\leq 20\%$ with respect to the base peak were omitted.